Distributed Control of Multizone HVAC Systems Considering Indoor Air Quality

Yu Yang, *Student Member, IEEE*, Seshadhri Srinivasan, *Senior Member, IEEE*, Guoqiang Hu, *Senior Member, IEEE*, and Costas J. Spanos, *Fellow, IEEE*

***Abstract*— This article studies a scalable control method for multizone heating, ventilation, and air-conditioning (HVAC) systems to optimize the energy cost for maintaining thermal comfort (TC) and indoor air quality (IAQ) (represented by CO_2) simultaneously. This problem is computationally challenging due to the complex system dynamics, various spatial and temporal couplings, as well as multiple control variables to be coordinated. To address the challenges, we propose a two-level distributed method (TLDM) with an upper level and lower level control integrated. The upper level computes zone mass flow rates for maintaining zone TC with minimal energy cost, and then, the lower level strategically regulates zone mass flow rates and the ventilation rate to achieve IAQ while preserving the near energy-saving performance of upper level. As both the upper and the lower level computation are deployed in a distributed manner, the proposed method is scalable and computationally efficient. The near-optimal performance of the method in energy cost saving is demonstrated through comparison with the centralized method. In addition, the comparisons with the existing distributed method show that our method can provide IAQ with only little increase of energy cost, while the latter fails. Moreover, we demonstrate that our method outperforms the demand-controlled ventilation (DCVs) strategies for IAQ management with about 8%–10% energy cost reduction. *Note to Practitioners:* The high portion of building energy consumption has motivated the energy saving for heating, ventilation, and air-conditioning (HVAC) systems. Concurrently, the living standards for indoor environment are rising among the occupants. Nevertheless, the status quo on improving building energy efficiency has mostly focused on maintaining thermal comfort (such as temperature), and the indoor air quality (IAQ) (usually represented by CO_2 level) has been seldom incorporated. In our previous work with the similar setting, we observed that the CO_2 levels will surge beyond tolerance during the high occupancy periods if only thermal comfort (TC) is considered for HVAC control. This deduces the IAQ and TC should be jointly considered while pursuing the energy cost saving target and thus studied in this article. This task is computationally cumbersome due to the complex system dynamics (thermal and CO_2) and tight correlations among the different control components (variable air volume and fresh air damper). To cope with these challenges, this work develops a two-level distributed computation paradigm for HVAC systems based on problem structures. Specifically, the upper level control (ULC) first calculates zone mass flow rates for maintaining comfortable zone temperature with minimal energy cost, and then, the lower level strategically regulates the computed zone mass flow rates as well as ventilation rate to satisfy IAQ while preserving the near energy-saving performance of the ULC. As both the upper and lower level calculations can be implemented in a distributed manner, the proposed method is scalable to large multizone deployment. The method's performance both in maintaining comfort (i.e., TC and IAQ) and energy cost saving is demonstrated via simulations in comparisons with the centralized method, the distributed token-based scheduling strategy, and the demand-controlled ventilation strategies.**

***Index Terms*— CO_2, distributed approach, indoor air quality (IAQ), multizone heating, ventilation, and air-conditioning (HVAC) system, two levels.**

I. Introduction

THE heating, ventilation, and air-conditioning (HVAC) systems account for 40%–50% of building energy consumption for maintaining comfortable indoor environment [1]. Aware of the high portion of energy consumption, the proposition to improve energy efficiency for HVAC systems has stimulated widespread attention [2], [3]. A plenty of works have demonstrated that substantial energy can be saved by deploying advanced HVAC control strategies (see [4], [5]). However, regarding the human sensation, the main focus has been placed on thermal comfort (TC) that is usually indicated by temperature and humidity [6], [7], and the indoor air quality (IAQ), such as the carbon dioxide (CO_2) concentration, has been seldom studied.

IAQ is closely related to the mechanical ventilation rate (i.e., fresh air infusion) of HVAC systems, especially nowadays where most buildings are constructed in closed envelope for energy-saving concerns. IAQ has emerged as a critical issue along developing building automation. On the one hand, the living standards and awareness of health are rising among the occupants; on the other hand, IAQ is closely related to occupant well-being and working productivity [8], [9]. A study conducted by the National Institute of Environmental Health Science (NIEHS) in 2015 has demonstrated the impact of IAQ

Manuscript received February 17, 2020; revised August 19, 2020; accepted September 27, 2020. Manuscript received in final form December 23, 2020. This work was supported by the Republic of Singapore's National Research Foundation through a grant to the Berkeley Education Alliance for Research in Singapore (BEARS) for the Singapore-Berkeley Building Efficiency and Sustainability in the Tropics (SinBerBEST) Program. Recommended by Associate Editor A. Marino. *(Corresponding author: Yu Yang.)*

Yu Yang and Seshadhri Srinivasan are with SinBerBEST, Berkeley Education Alliance for Research in Singapore, Singapore 138602 (e-mail: yu.yang@bears-berkeley.sg; seshadhri.srinivasan@bears-berkeley.sg).

Guoqiang Hu is with the School of Electrical and Electronic Engineering, Nanyang Technological University, Singapore 639798 (e-mail: gqhu@ntu.edu.sg).

Costas J. Spanos is with the Department of Electrical Engineering and Computer Sciences, University of California at Berkeley, Berkeley, CA 94720 USA (e-mail: spanos@berkeley.edu).

Color versions of one or more figures in this article are available at https://doi.org/10.1109/TCST.2020.3047407.

Digital Object Identifier 10.1109/TCST.2020.3047407

on cognitive abilities [10]. Significantly, the findings show that the strategic skills of occupants reduce to 20% with an indoor CO_2 concentration 1400 ppm compared to the normal outdoor level of 400 ppm. Straightforwardly, for energy-efficient HVAC control, as the TC only relates to zone mas flow rates, the fresh air ventilation of HVAC systems is usually suppressed to the lower boundary to minimize the cooling load. However, for IAQ management, sufficient ventilation is required to dilute the indoor air. This implies considering TC alone is not enough for developing energy-efficient HVAC control strategies. As in such setting, the energy-saving target may be achieved at the expense of awful IAQ. Specifically, we can imagine that the CO_2 concentration will accumulate and surge beyond tolerance during the time periods with high occupancy though the temperature is maintained comfortable if sufficient fresh air ventilation is not provided by the HVAC systems.

Notably, increasing focus has been shifted toward IAQ management for HVAC systems both from industries and research communities in recent years. Some industries have informed that the thermostats will integrate CO2 sensors inside for monitoring IAQ in foreseeable future [11]. Within the research communities, some pioneering works have jointly considered IAQ and TC while studying energy-efficient HVAC control (see [12]–[14]). Nevertheless, this problem has not been well addressed yet as: 1) the related works are still fairly limited (see the references therein) and 2) most of them are for single-zone cases [12], [13] or not scalable to multizone commercial buildings due to the centralized computation framework [14]. The computational challenges of the complex problem remain to be addressed.

1) Multiple control variables need to be coordinated for achieving the multiple objectives. Both the ventilation rate and zone mass flow rates require to be coordinated to optimize energy efficiency for achieving TC and IAQ simultaneously. In particular, a good IAQ requires a high ventilation rate and zone mass flow rates. However, this may induce lower temperature bound violations and high energy cost.
2) The problem is nonlinear and nonconvex due to the complex system dynamics. Both the energy cost and system dynamics (i.e., temperature and CO_2) are nonlinear with respect to the control inputs: zone mass flow rates and ventilation rate.
3) There exist various spatial and temporal couplings. The optimal operation of HVAC systems should consider zone temperature and CO_2 inertia, which corresponds to substantial temporal constraints. Besides, the interzone heat transfer and the recirculated air to AHU induce tight spatial couplings.

A. Contributions

Motivated by the literature, this article studies the control of multizone commercial HVAC systems to optimize the energy cost for maintaining TC and IAQ simultaneously. We make the following contributions to overcome the computational challenges.

(C1) We propose a two-level control method integrated with the upper level control (ULC) and the lower level control (LLC) by exploiting the problem structures.
(C2) While the ULC adopts an existing distributed method, we develop a distributed method for the LLC to achieve scalability and computation efficiency.
(C3) We demonstrate the method's performance in energy cost saving, human comfort (i.e., temperature and CO_2), as well as computation efficiency through simulations.

Our two-level structure is motivated by the independent zone temperature and zone CO_2 dynamics (but both subject to the control inputs), which makes it possible to tackle the two comfort indexes successively. Therefore, we decompose the problem into two levels: the ULC first computes the optimal zone mass flow rates for maintaining zone TC with minimal energy cost. Successively, the LLC strategically regulates the computed zone mass flow rates from ULC and ventilation rate to achieve the desirable IAQ. Such a two-level paradigm makes it computationally tractable to achieve the two comfort indexes simultaneously while preserving the near-optimal energy cost. Moreover, the two-level structure favors computation efficiency as the LLC is only invoked when the CO_2 upper bounds are to be violated. In particular, as the ULC on TC has been comprehensively studied in our previous work [15] and thus adopted, we place our main focus on bringing in the two-level structure and the LLC.

The remainder of this article is structured as follows. In Section II, we review the related works. In Section III, we present the problem formulation. In Section IV, we discuss the two-level distributed method (TLDM). In Section V, we evaluate the performance of the method via simulations. In Section VI, we briefly conclude this article.

II. Related Works

Developing advanced control for HVAC systems to improve energy efficiency has been an edge issue along building automation over the past decades. Various methods have been studied, and some comprehensive reviews can refer to [2] and [3]. Significantly, these existing works have proved that substantial energy can be saved by deploying advanced HVAC control while not compromising human comfort. From the computation structure standpoint, these methods can be categorized into centralized methods [4] and decentralized methods [5]. Centralized approaches are usually developed for single-room/zone cases and not amenable to commercial buildings due to the substantial computation burden (see [6], [7]). By contrast, a number of decentralized approaches have been developed to address the computation challenges of commercial HVAC systems [5], [15], [16].

Nevertheless, one critical issue to be noticed is that most of these works have focused on TC (i.e., temperature, humidity, and so on) and lack IAQ management while pursuing energy cost savings (see [17], [18], and the references therein). In this backdrop, the IAQ may be awful and beyond tolerance though the temperature is maintained comfortably. For example, the pollutants and particles, especially CO_2 concentration, accumulate over the time if sufficient ventilation

(i.e., outdoor fresh air) is not provided. This is easy to understand as high proportion of recirculated air is preferred to reduce the cooling load. In the literature, the IAQ management is mostly addressed by some simple ventilation rules referred to the demand-controlled ventilation (DCV) strategies. Such methods could be CO_2-based [19]–[21] or occupancy-based [22]–[24]. The main ideas are adjusting the amounts of fresh air infusion based on the detected instantaneous CO_2 concentration or occupancy, whereas for multizone commercial buildings, the DCVs tend to cause overventilation or underventilation due to zone CO_2 or occupancy variations [25]. Another drawback is that the ventilation regulation for IAQ management is not coordinated with the TC, which will jeopardize the energy-saving objective of HVAC systems.

It is imperative to jointly consider both TC and IAQ simultaneously for achieving HVAC energy cost savings and maintaining human comfort. Such awareness has motivated the joint management of TC and IAQ for single-zone cases [12], [13], [26]. In particular, most of these methods depend on simplified linear models to capture system dynamics. Therefore, the methods and modelings are generally not amenable to multizone commercial buildings. As a scarce exception, Yu *et al.* [14] studied both TC and IAQ management for commercial HVAC systems based on the Lyapunov optimization. The performance of the method both in maintaining human comfort (i.e., TC and IAQ) and saving energy cost was demonstrated in a four-zone case study. However, the computation tractability for larger-scale applications remains to be addressed and motivates this work.

III. Problem Formulation

A. HVAC Systems for Commercial Buildings

The configuration for a typical commercial HVAC system is shown in Fig. 1, which mainly consists of an air handling unit (AHU), variable air volume (VAV) boxes, and a chiller system (not shown here). The AHU is basically integrated with a damper, a cooling/heating coil, and a supply fan. The heating/cooling coil cools down/heats up the mixed air (the mixture of outside fresh air and inside recirculated air) to the set-point temperature. The damper regulates the ventilation rates: the fraction of recirculated air d_r or the fraction of outdoor fresh air $1-d_r$. Therefore, a smaller d_r specifies a higher proportion of fresh air infusion but induces higher cooling demand for the HVAC system and vice versa. The supply fan is for driving the circulation of air within the building duct network. As another main component, the VAV boxes are connected to the zones, each of which consists of a damper and a heating coil. The damper regulates the zone mass flow rate and the heating coil reheats the supply air if necessary (not discussed in this article). The chiller system is usually constituted by a chiller pump, water tank, and the chiller, which provides continuous chilled water to the cooling coils of AHU. Except for the chiller, the chiller pump is also partially responsible for the HVAC's energy consumption for circulating the water between the water tank and the chiller. This article studies HVAC systems with constant water flow system [27] where the chiller pump's energy consumption can

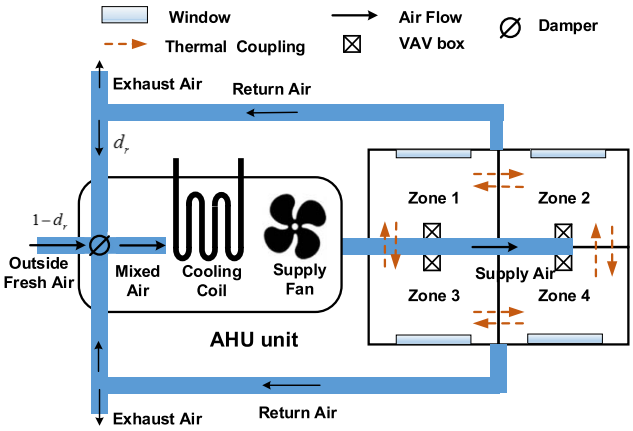

Fig. 1. Schematic of the HVAC system for multizone buildings.

be regarded as fixed and thus not explicitly discussed. Besides, without loss of generality, this article studies the cooling mode. More details of the HVAC systems can refer to [4] and [28].

As aforementioned, we seek to minimize the energy cost for maintaining both zone TC and IAQ simultaneously. In such a setting, both zone air flow rates and ventilation rate (d_r) need to be coordinated. The problem is studied in a discrete-time framework on a daily basis with $\Delta_k = 30$ min's sampling and computing epoch. To account for the multistage control under uncertainties (e.g., weather, occupancy, and so on), we deploy the model predictive control (MPC) framework: the control inputs at each executed epoch are computed based on the predicted information over a look-ahead planning horizon $H = 10$ (5 h). This process is repeated with the time evolving until the end of the optimization horizon $\mathcal{T}$.

B. Zone Thermal Dynamics

We consider a commercial building with I zones indexed by $\mathcal{I} = \{1, 2, \ldots, I\}$. At each computing epoch, the zone thermal dynamics over the planning horizon $\mathcal{H} = \{0, 1, \ldots, H-1\}$ are captured by a resistance–capacitance (RC) network [29], [30]

$$\begin{aligned} C_i^{\rho}(T_i(k+1) - T_i(k)) &= \sum_{j\in\mathcal{N}_i} \frac{T_j(k) - T_i(k)}{R_{ij}}\Delta_k + \frac{T_o(k) - T_i(k)}{R_{oi}}\Delta_k \\ &\quad + c_p m_i^z(k)(T_c - T_i(k))\Delta_k + Q_i(k)\Delta_k \quad \forall i \in \mathcal{I}, k \in \mathcal{H} \end{aligned} \tag{1}$$

where $k \in \mathcal{H}$ and $i, j \in \mathcal{N}$ denote the time and zone indices, respectively. C_i^{ρ} is the zone air heat capacity. $T_i(k)$, $T_o(k)$, and T_c denote the zone temperature, outdoor temperature, and the set-point temperature of AHU, respectively. R_{ij} (R_{ji}) denotes the adjacent zone thermal resistance. In particular, R_{oi} denotes the thermal resistance between zone i and the outside, We use $\mathcal{N}_i$ to indicate the set of spatially adjacent zones to zone i. c_p is the specific heat of the air. $m_i^z(k)$ indicates the zone mass flow rate. $Q_i(k)$ captures zone internal heat gains from the occupants and electrical equipment, which can be estimated by the occupancy [31].

We translate (1) into a standard form

$$T_i(k+1) = A_{ii}T_i(k) + \sum_{j\in\mathcal{N}_i} A_{ij}T_j(k) + C_{ii}m_i^z(k)(T_i(k) - T_c) + D_i(k) \ \forall i \in \mathcal{I}, k \in \mathcal{H}. \tag{2}$$

where $A_{ii} = 1 - (\sum_{j\in\mathcal{N}_i} \Delta_k/(R_{ij}C_i^\rho) + \Delta_k/(C_i^\rho R_{oi}))$, $A_{ij} = \Delta_k/(C_i^\rho R_{ij})$, $C_{ii} = -(\Delta_k \cdot c_p)/C_i^\rho$, and $D_i(k) = (\Delta_k T_o(k))/(C_i^\rho R_{oi}) + (\Delta_k \cdot Q_i(k))/(C_i^\rho)$.

Similar to [12] and [14], this article uses CO_2 concentration as an IAQ indicator. The zone CO_2 dynamics for multizone commercial buildings can be described by [14]

$$m_i(C_i(k+1) - C_i(k)) = N_i(k)C_g\Delta_k + m_i^z(k)(C_z(k) - C_i(k))\Delta_k \quad \forall i \in \mathcal{I}, \quad k \in \mathcal{H} \tag{3}$$

where m_i denotes zone air mass and $C_i(k)$ (in ppm) denotes zone CO_2 concentration. We suppose that the occupants are the main source of CO_2 generation, and thus, the CO_2 accumulation can be estimated by the average CO_2 generation rate per person C_g ($\mathrm{g\,h^{-1}}$) multiplied by the occupancy $N_i(k)$ as indicated in the first term of right-hand side. $C_z(k)$ denotes the CO_2 concentration of supply air, which can be estimated by

$$C_z(k) = (1 - d_r(k))C_o(k) + d_r(k)C_{\mathrm{m}}(k), \quad \text{with } C_{\mathrm{m}}(k) = \frac{\sum_{i\in\mathcal{I}} m_i^z(k)C_i(k)}{\sum_{i\in\mathcal{I}} m_i^z(k)} \quad \forall k \in \mathcal{H} \tag{4}$$

where $d_r(k) \in [0, 1]$ denotes the fraction of return air delivered to AHU (i.e., the ventilation rate to be controlled). $C_m(k)$ characterizes the average CO_2 concentration of the return air from all zones.

From (3) and (4), we note that the zone CO_2 dynamics are nonlinear and fully coupled through the recirculated air.

C. Decision Variables

Our objective is to minimize the HVAC energy cost for maintaining TC and IAQ. Therefore, our decision variables can be divided into control variables and state variables. The control variables are the control inputs of the HVAC system that affects indoor condition, which includes the ventilation rate $d_r(k)$ and zone mass flow rate $m_i^z(k)$. Our state variables are zone temperature $T_i(k)$ and zone CO_2 concentration $C_i(k)$, which indicates human comfort and requires to be maintained.

D. Objective Function

The energy consumption of the HVAC system is mainly incurred by the cooling coil $P_f(k)$ and supply fan $P_f(k)$ within AHU, that is

$$P_c(k) = c_p\eta(1 - d_r(k))\sum_{i\in\mathcal{I}} m_i^z(k)(T_o(k) - T_c) + c_p\eta d_r(k)\sum_{i\in\mathcal{I}} m_i^z(k)(T_i(k) - T_c)$$
$$P_f(k) = \kappa_f\left(\sum_{i\in\mathcal{I}} m_i^z(k)\right)^2 \tag{5}$$

where η is the reciprocal of the coefficient of performance (COP) of the chiller, which captures the ratio of provided cooling to the total consumed electrical power.

Considering that the energy consumption is not easy to inspect in practice, we selected the total energy cost charged by the electricity price c_k (s$/kW) on a daily basis as our objective

$$J = \sum_{k\in\mathcal{H}} c_k\big(P_c(k) + P_f(k)\big)\Delta_k. \tag{6}$$

E. System Constraints

The HVAC operation should respect the TC and IAQ requirements, which are represented by zone temperature bounds [5] and CO_2 bounds [14] in this article

$$T_i^{\min} \le T_i(k) \le T_i^{\max} \quad \forall i \in \mathcal{I}, \ k \in \mathcal{H} \tag{7}$$
$$C_i(k) \le C_i^{\max} \quad \forall i \in \mathcal{I}, \ k \in \mathcal{H} \tag{8}$$

where $T_i^{\min}$ and $T_i^{\max}$ characterize the comfortable zone temperature ranges. $C_i^{\max}$ denotes the desirable zone CO_2 upper bound. In particular, the formulation can account for personalized human comfort by differentiating $T_i^{\min}$, $T_i^{\max}$, and $C_i^{\max}$ with respect to the zones.

In addition, the HVAC operation must abide by the physical limits of VAV boxes and AHU

$$m_i^{z,\min} \le m_i^z(k) \le m_i^{z,\max} \quad \forall i \in \mathcal{I}, \ k \in \mathcal{H} \tag{9}$$
$$\sum_{i\in\mathcal{I}} m_i^z(k) \le m^{\max} \quad \forall k \in \mathcal{H} \tag{10}$$

where $m_i^{z,\min}$ and $m_i^{z,\max}$ denote the operation range of VAV boxes and $m^{\max}$ denotes the supply capacity of AHU.

Similarly, the damper of AHU for regulating ventilation rate is usually restricted to the operation range characterized by $d_r^{\min}$ and $d_r^{\max}$ to reduce wear and tear

$$d_r^{\min} \le d_r(k) \le d_r^{\max} \quad \forall k \in \mathcal{H}. \tag{11}$$

F. Problem

Overall, the optimization problem at each computing epoch can be summarized as ($\mathcal{P}$)

$$\min_{\boldsymbol{m}_i^z, \boldsymbol{T}_i, \boldsymbol{C}_i, i \in \mathcal{I}, \boldsymbol{d}_r} J \quad \text{s.t.} \quad (2) - (4), (7) - (8), \ (9) - (10), \ (11) \tag{$\mathcal{P}$}$$

where we have $\boldsymbol{m}_i^z = [m_i^z(k)]_{k\in\mathcal{H}}$, $\boldsymbol{T}_i = [T_i(k)]_{k\in\mathcal{H}}$, $\boldsymbol{C}_i = [C_i(k)]_{k\in\mathcal{H}}$ ($\forall i \in \mathcal{I}$), and $\boldsymbol{d}_r = [d_r(k)]_{k\in\mathcal{H}}$ denoting the concatenating decision variables over the computing epoch.

It is clear to see that problem ($\mathcal{P}$) is nonlinear and nonconvex. The nonlinearity and nonconvexity both arise from the objective function and the constraints. Moreover, the substantial spatially and temporally coupled constraints imposed by zone temperature and zone CO_2 make it computationally intractable even for moderate commercial HVAC systems with centralized methods. Indeed, this motivates our TLDM to be discussed.

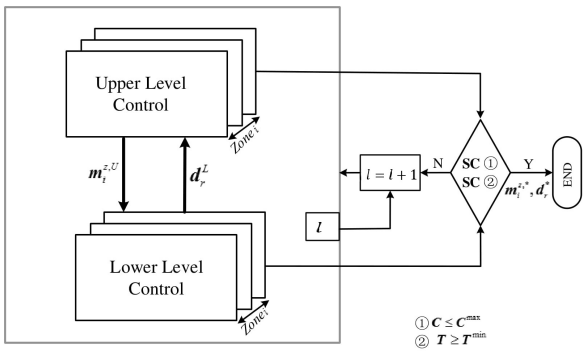

Fig. 2. Framework of TLDM.

IV. TLDM

To address the computational challenges of problem $(\mathcal{P})$, we propose a TLDM based on the problem structures: the zone temperature and CO_2 dynamics are independent (but both subject to the control inputs). We divide the problem into two levels: the ULC and the LLC. The ULC is mainly responsible for TC, and the LLC corresponds to IAQ management. The underlying idea of the two-level structure is to address the two comfort indexes successively while preserving the near-optimal energy-saving performance. Moreover, such two-level structure favors computation efficiency as the LLC requires to be invoked only if CO_2 is to be violated. Both the ULC and the LLC use distributed implementation to achieve scalability and computation efficiency. We present the holistic framework of the TLDM in Fig. 2. In particular, the ULC first computes the zone flow rates $\boldsymbol{m}^{z,U}$ for maintaining TC with minimal energy cost, and then, the LLC strategically regulates the ventilation rate $\boldsymbol{d}_r^L$ to achieve IAQ while preserving the near energy cost of ULC. The ULC and LLC alternate and communicate with each other. The implementation of ULC and LLC is as follows.

A. ULC

The ULC focuses on maintaining zone TC with minimal energy cost. Considering that zone temperature is only affected by zone mass flow rate $m_i^z(k)$ and the HVAC's energy cost is nondecreasing with respect to the ventilation rate $d_r(k)$, we define the ULC problem as

$$\begin{aligned} \min_{\boldsymbol{m}_i^z, \boldsymbol{T}_i, i \in \mathcal{I}.} \quad & J^U \\ \text{s.t.} \quad & (2), (7), (9) - (10). \\ & d_r(k) = d_r^L(k), k \in \mathcal{H} \end{aligned} \tag{$\mathcal{P}_U$}$$

where we have $J^U = J$ and $\boldsymbol{d}_r^L = [d_r^L(k)]_{k \in \mathcal{K}}$. The intuitive interpretation of ULC is to identify the zone mass flow rates for maintaining TC with minimal energy cost under the specified ventilation rate $d_r^L(k)$ from LLC [we can start with $d_r^{\max}$ $(k \in \mathcal{H})$]. For problem $(\mathcal{P}_U)$, there already exists a number of distributed methods [5], [15]. We adopt our previously proposed distributed method [15] and place our main attention on the implementation of LLC.

B. LLC

As shown in Fig. 2, the LLC only needs to be invoked when the zone CO_2 concentrations violate the upper bounds (i.e., $C_i(k) \ge C_i^{\max}$). Clearly, both increasing zone mass flow rates and ventilation rate [decrease $d_r(k)$] can dilute zone CO_2 and thus improve IAQ. However, the latter is generally more expensive as it increases the cooling load of all zones. With the concern to preserve the near energy cost computed in ULC, our LLC adopts a two-phase method to achieve IAQ. We first seek to regulate zone mass flow rates to satisfy the user-defined zone CO_2 bounds. To preserve the near energy cost of ULC, we select the deviation of zone mass flow rates relative to the ULC calculations as the objective. We have the following problem for the first phase of LLC:

$$\begin{aligned} \min_{\boldsymbol{m}_i^z, \boldsymbol{C}_i, i \in \mathcal{I}.} \quad & J^L = \sum_{k \in \mathcal{H}} \sum_{i \in \mathcal{I}} \left(m_i^z(k) - m_i^{z,U}(k) \right)^2 \\ \text{s.t.} \quad & m_i^{z,U}(k) \le m_i^z(k) \le m_i^{z,\max} \quad \forall i \in \mathcal{I} \\ & (3) - (4), (8), (10) \end{aligned} \tag{$\mathcal{P}_L$}$$

(12)

where constraints (3), (4), and (8) capture zone CO2 dynamics and bounds. Constraint (10) denotes the supply capacity of AHU. In particular, constraint (12) models the zone mass flow rate lower bounds for maintaining TC, which is obtained from the ULC.

We suppose to achieve TC and IAQ simultaneously by solving problem $(\mathcal{P}_L)$, and however, things may not always happen in that way. We note that only the upper comfortable zone temperature bounds can be maintained but not necessarily the lower ones by (12). Therefore, it may occur that the desirable CO_2 is achieved by solving problem $(\mathcal{P}_L)$, but the zone temperature drops beyond the lower bounds due to the substantial increase of zone mass flow rates. Actually, this means that regulating zone mass flow rates alone is not viable to achieve the two comfort indexes simultaneously, and the second phase of LLC should be invoked to increase the ventilation rate (decrease $\boldsymbol{d}_r$). As shown in Fig. 2, such two phases alternate until we achieve the two comfort indexes. Suppose that the two-phase structure gets well across, and the remaining problem is about the implementation.

First Phase of LLC: Clearly, for the first phase, we require to solve the nonlinear and nonconvex problem $(\mathcal{P}_L)$, which is a nontrivial task. We note that the zone CO_2 dynamics are fully coupled through the recirculated air, posing the primary challenge to develop a distributed method. To handle this, we introduce a learning framework to estimate CO_2 concentration for the supply air $C_z(k)$. Therefore, the procedure to solve problem $(\mathcal{P}_L)$ contains two successive steps: first estimate $C_z(k)$ and then solve problem of $(\mathcal{P}_L)$ with the estimated $C_z(k)$. Specifically, with the estimated $\boldsymbol{C}_z(k)$, we have the decoupled zone CO_2 dynamics

$$\begin{aligned} C_i(k+1) = & C_i(k) + E_i(k) m_i^z(k) \\ & + F_i(k) m_i^z(k) C_i(k) + G_i(k) \end{aligned} \tag{13}$$

where $E_i(k) = C_z(k)\Delta_k / m_i$, $F_i(k) = -\Delta_k / m_i$, and $G_i(k) = N_i(k) C_g \Delta_k / m_i$ are now constant parameters.

We note that the zone CO_2 dynamics (13) are bilinear with respect to the zone mass flow rate $m_i^z(k)$ and

zone CO_2 $C_i(k)$. To address the nonlinearity, we introduce some auxiliary decision variables $Z_i(k) = m_i^z(k)C_i(k)$ and use the McCormick envelopes [32] to relax the bilinear terms

$$Z_i(0) = m_i^z(0)C_i(0) \tag{13a}$$
$$Z_i(k) \geq m_i^{z,\min}C_i(k) + m_i^z(k)C_i^{\min} - m_i^{z,\min}C_i^{\min} \tag{13b}$$
$$Z_i(k) \geq m_i^{z,\max}C_i(k) + m_i^z(k)C_i^{\max} - m_i^{z,\max}C_i^{\max} \tag{13c}$$
$$Z_i(k) \leq m_i^z(k)C_i^{\max} + m_i^{z,\min}C_i(k) - m_i^{z,\min}C_i^{\max} \tag{13d}$$
$$Z_i(k) \leq m_i^{z,\max}C_i(k) + m_i^z(k)C_i^{\min} - m_i^{z,\max}C_i^{\min} \tag{13e}$$
$$\forall k \in \mathcal{H} \setminus \{0\} \tag{14}$$

where $C_i(0)$ denotes the measured zone CO_2 at the beginning of current computing epoch.

By invoking the auxiliary decision variables $Z_i(k)$, we have the following relaxed convex problem for problem $(\mathcal{P}_L)$:

$$\min_{\boldsymbol{m}_i^z, \boldsymbol{C}_i, \boldsymbol{Z}_i, \forall i \in \mathcal{I}.} \quad J^L = \sum_{k\in\mathcal{H}}\sum_{i\in\mathcal{I}}\left(m_i^z(k) - m_i^{z,U}(k)\right)^2 \tag{$\mathcal{P}'_L$}$$
$$\text{s.t.} \quad C_i(k+1) = C_i(k) + E_i(k)m_i^z(k) + F_i(k)Z_i(k) + G_i(k) \quad \forall i \in \mathcal{I},\ k \in \mathcal{H}$$
$$(8), (10), (12), (13a) - (13e). \tag{14a}$$

We note that problem $(\mathcal{P}'_L)$ is characterized by: 1) a decomposable objective function with respect to the zones and 2) coupled linear constraints. This problem can be efficiently tackled by the accelerated distributed augmented Lagrangian (ADAL) method [33], which may be more clearly seen by recasting it into a standard form

$$\min_{\boldsymbol{x}_i, i\in\mathcal{I}} \quad J^L = \sum_{i\in\mathcal{I}} J_i^L(\boldsymbol{x}_i)$$
$$\text{s.t.} \quad \sum_{i=0}^{I} \boldsymbol{A}_i^c\boldsymbol{x}_i = \boldsymbol{b}^c \tag{$\mathcal{P}''_L$}$$
$$\boldsymbol{x}_i \in \boldsymbol{X}_i \quad \forall i \in \mathcal{I}\cup\{0\}$$

where $\boldsymbol{x}_i = [(\boldsymbol{x}_i(k))^T]_{k\in\mathcal{H}}^T$ and $\boldsymbol{x}_i(k) = (C_i(k), m_i^z(k), Z_i(k))^T$ concatenating the decision variables of zone i. $J_i^L(\boldsymbol{x}_i) = \sum_{k\in\mathcal{H}}(m_i^z(k) - m_i^{z,U}(k))^2$ represents the local objective function of zone i. $\sum_{i=0}^{I}\boldsymbol{A}_i^c\boldsymbol{x}_i = \boldsymbol{b}^c$ accounts for the coupled linear constraints (10) with an additional slack variables $\boldsymbol{x}_0(k) \geq 0$ introduced at each stage (transform the inequality constraints to equality constraints). $\boldsymbol{X}_i$ $(\forall i \in \mathcal{I})$ indicates the local constraints (8), (12), and (13a)–(13e) corresponding to zone i and particularly $\mathcal{X}_0 = \{\boldsymbol{x}_0 | \boldsymbol{x}_0 \geq \boldsymbol{0}\}$. We have

$$\boldsymbol{A}_i^c = \begin{pmatrix} 0 & 1 & 0 & 0 & 0 & 0 & \cdots \\ 0 & 0 & 0 & 0 & 1 & 0 & \cdots \\ \cdots & \cdots & \cdots & \cdots & \cdots & \cdots & \cdots \end{pmatrix} \in \mathbb{R}^{H\times 3H} \quad (\forall i \in \mathcal{I})$$

and $\boldsymbol{b}^c = (m^{\max}, m^{\max}, \ldots, m^{\max})^T \in \mathbb{R}^H$.

Following the standard procedure of ADAL [33], we have the augmented Lagrangian function:

$$\mathbb{L}_\rho(\boldsymbol{x}_0, \boldsymbol{x}_1, \ldots, \boldsymbol{x}_I, \boldsymbol{\alpha}) = \sum_{i\in\mathcal{I}} J_i^L + \boldsymbol{\alpha}^T\left(\sum_{i=0}^{I}\boldsymbol{A}_i^c\boldsymbol{x}_i - \boldsymbol{b}^c\right) + \frac{\rho}{2}\left\|\sum_{i=0}^{I}\boldsymbol{A}_i^c\boldsymbol{x}^i - \boldsymbol{b}^c\right\|^2 \tag{16}$$

where $\boldsymbol{\alpha} = (\alpha_0, \alpha_1, \ldots, \alpha_{H-1})^T$ are Lagrangian multipliers and $\rho(\rho > 0)$ is penalty parameter.

Therefore, we have the following primal problem with given Lagrangian multipliers $\boldsymbol{\alpha}$:

$$\min_{\boldsymbol{x}_0, \boldsymbol{x}^i, \forall i\in\mathcal{I}} \quad \mathbb{L}_\rho(\boldsymbol{x}_0, \boldsymbol{x}_1, \ldots, \boldsymbol{x}_I, \boldsymbol{\alpha})$$
$$\text{s.t.} \quad \boldsymbol{x}_i \in \mathcal{X}_i \quad \forall i \in \mathcal{I}.$$
$$\boldsymbol{x}_0 \geq \boldsymbol{0}. \tag{17}$$

The main procedures of using ADAL to solve problem $(\mathcal{P}''_L)$ generally contain three steps: 1) solving the primal problem (17); 2) updating the Lagrangian multipliers $\boldsymbol{\alpha}$; and 3) updating the penalty factor ρ. While the last two procedures are standard, we illustrate how to solve the primal problem $(\mathcal{P}''_L)$ in a distributed fashion. Specifically, we define $I+1$ agents, where Agent $1 \sim I$ corresponds to the I zones and Agent 0 is a virtual agent for managing the slack decision variable $\boldsymbol{x}_0$. At each iteration q, we have the local objective functions the agents

$$\mathbb{L}_\rho^0(\boldsymbol{x}_0, \boldsymbol{x}_{-0}^q, \boldsymbol{\alpha}) = \boldsymbol{\alpha}^T\boldsymbol{A}_0^c\boldsymbol{x}_0 + \frac{\rho}{2}\left\|\boldsymbol{A}_0^c\boldsymbol{x}_0 + \sum_{i=1}^{I}\boldsymbol{A}_i^c\boldsymbol{x}_i^q - \boldsymbol{b}^c\right\|^2$$
$$\mathbb{L}_\rho^i(\boldsymbol{x}_i, \boldsymbol{x}_{-i}^q, \boldsymbol{\alpha}) = J_i^L + \boldsymbol{\alpha}^T\boldsymbol{A}_i^c\boldsymbol{x}_i + \frac{\rho}{2}\left\|\boldsymbol{A}_i^c\boldsymbol{x}_i + \sum_{j\in\mathcal{I}\cup\{0\}, j\neq i}\boldsymbol{A}_j^c\boldsymbol{x}_j^q - \boldsymbol{b}^c\right\|^2 \quad \forall i \in \mathcal{I}.$$

It is clear that we can obtain the estimated zone mass flow rates $m_i^z(k)$ and zone CO_2 $C_i(k)$ by solving problem $(\mathcal{P}''_L)$. Afterward, we invoke the procedure to update the estimation of $C_z(k)$ according to (4).

Overall, we present the details to solve problem $(\mathcal{P}_L)$ based on ADAL in Algorithm 1. We use the superscripts p and q to denote the iteration corresponding to solving the relaxed problem $(\mathcal{P}''_L)$ and updating the estimation of $C_z(k)$, respectively. For notation, $\boldsymbol{x}^q = [(\boldsymbol{x}_j^q)^T]_{j\in\mathcal{I}\cup\{0\}}^T$ represent the augmented control and state trajectories for all agents, while $\boldsymbol{x}_{-i}^q = [(\boldsymbol{x}_j^q)^T]_{j\in\mathcal{I}\{0\}, j\neq i}^T$ excluding Agent i. For the ADAL method, we use the residual error of coupled constraints: $r_q(\boldsymbol{x}) = \|\sum_{i=0}^{I}\boldsymbol{A}_i^c\boldsymbol{x}_i^q - \boldsymbol{b}^c\| \leq \epsilon^{\text{in}}$ **(C1)** as the stopping criterion. For the estimation of CO_2 concentration for the supply air, we evaluate the deviations of any two successive estimation: $\|\boldsymbol{C}_z^{p+1} - \boldsymbol{C}_z^p\| \leq \epsilon^{\text{out}}$ **(C2)**, where ϵ^{in} and ϵ^{out} are small positive thresholds.

Recursive Feasibility: Recall that the bilinear terms $Z_i(k) = m_i^z(k)C_i(k)$ are relaxed in problem $(\mathcal{P}'_L)$ (or $(\mathcal{P}''_L)$), and therefore, the recursive feasibility remains to be addressed. We propose a heuristic method (see Algorithm 2) to recover a control input $\hat{\boldsymbol{x}} = [(\hat{\boldsymbol{x}}_i(k))^T]_{k\in\mathcal{H}}^T$ from the optimal solution of problem $(\mathcal{P}''_L)$, which can ensure the recursive feasibility and near energy-saving performance. The main idea is to preserve the computed zone mass flow rates: $\hat{m}_i^z(k) = m_i^{z,*}(k)$ $(\forall i \in \mathcal{I}, k \in \mathcal{H})$ as they determine the HVAC's energy cost. In such a setting, the desirable CO_2 at each executed epoch t will be sustained. As the method is deployed in the MPC framework, the desirable CO_2 over the day (optimization horizon $\mathcal{T}$) will

Algorithm 1 Solve Problem $(\mathcal{P}_L'')$ Based on ADAL

1: **Initialize** $p \leftarrow 0$, $\boldsymbol{C}_z^0$ and $\boldsymbol{d}_r$.
2: **Initialize** $q \leftarrow 0$, $\boldsymbol{\alpha}^0$, and $\boldsymbol{x}_i^0$ $(\forall i \in \mathcal{I} \cup \{0\})$, $\boldsymbol{C}_z = \boldsymbol{C}_z^p$.
3: **for** $i \in \mathcal{I} \cup \{0\}$, **do**

$$\boldsymbol{x}_i^{q+1} = \arg\min_{\boldsymbol{x}_i} \mathbb{L}_\rho^i(\boldsymbol{x}_i, \boldsymbol{x}_{-i}^q, \boldsymbol{\alpha}^q) \quad s.t. \quad \boldsymbol{x}_i \in \mathcal{X}_i. \tag{18}$$

4: **end for**
5: Update the Lagrangian multipliers:

$$\boldsymbol{\alpha}^{q+1} = \boldsymbol{\alpha}^q + \rho\Big(\sum_{i=0}^{I} \boldsymbol{A}_i^c \boldsymbol{x}_i^{q+1} - \boldsymbol{b}^c\Big)$$

6: If (**C1**) is satisfied, stop with $\boldsymbol{x}^p = \boldsymbol{x}^{q+1}$, otherwise $q \rightarrow q+1$ and go to Step 3.
7: Estimate $\boldsymbol{C}_z^{p+1}$ according to

$$\boldsymbol{C}_z^{p+1} = (1 - \boldsymbol{d}_r)\boldsymbol{C}_o + \boldsymbol{d}_r \frac{\sum_{i\in\mathcal{I}} \boldsymbol{m}_i^{z,p} \boldsymbol{C}_i^p}{\sum_{i\in\mathcal{I}} \boldsymbol{m}_i^{z,p}}. \tag{19}$$

8: If (**C2**) is satisfied, stop with $\boldsymbol{x}^p$, otherwise set $p \rightarrow p+1$ and go to Step 2.

Output: $\boldsymbol{x}^* = [(\boldsymbol{x}_i^p(k))^T]_{k\in\mathcal{H}}^T$, $\boldsymbol{x}_i^p(k) = \big(C_i^p(k), m_i^{z,p}(k), Z_i^p(k)\big)^T$.

Algorithm 2 Recover Recursive Feasibility

Input: $\boldsymbol{x}^* = [(\boldsymbol{x}_i^p(k))^T]_{k\in\mathcal{H}}^T$, $\boldsymbol{x}_i^p(k) = \big(C_i^p(k), m_i^{z,p}(k), Z_i^p(k)\big)^T$ (from **Algorithm** 1).
1: Set $\hat{C}_i(0) = C_i(0)$ and $\hat{T}_i(0) = T_i(0)$ $(\forall i \in \mathcal{I})$.
2: **for** $k \in \mathcal{H}$ **do**
3: **for** $i \in \mathcal{I}$ **do**
4: Set $\hat{m}_i^z(k) = m_i^{z,*}(k)$ and $\hat{Z}_i(k) = \hat{m}_i^z(k)\hat{C}_i(k)$.
5: Estimate $\hat{C}_i(k+1)$ and $\hat{T}_i(k+1)$ by

$$\hat{C}_i(k+1) = \hat{C}_i(k) + \hat{E}_i(k)\hat{m}_i^z(k) + F_i(k)\hat{Z}_i(k) + G_i(k),$$
$$\hat{T}_i(k+1) = A_{ii}\hat{T}_i(k) + \sum_{j\in\mathcal{N}_i} A_{ij}\hat{T}_j(k) + C_{ii}\hat{m}_i^z(k)(\hat{T}_i(k) - T_c) + D_i(k),$$

with $\hat{E}_i^z(k) = \hat{C}_z(k)\Delta_t/m_i$, and $\hat{C}^z(k) = (1 - d_r^*(k))C_o(k) + d_r^*(k)\frac{\sum_{i\in\mathcal{I}} \hat{m}_i^z(k)\hat{C}_i(k)}{\sum_{i\in\mathcal{I}} \hat{m}_i^z(k)}, \forall i \in \mathcal{I}, k \in \mathcal{H}$.

6: **end for**
7: **end for**

Output: $\hat{\boldsymbol{m}}_i^z = [\hat{m}_i^z(k)]_{k\in\mathcal{H}}$, $\hat{\boldsymbol{C}}_i = [\hat{C}_i(k)]_{k\in\mathcal{H}}$, and $\hat{\boldsymbol{T}}_i = [\hat{T}_i(k)]_{k\in\mathcal{H}}$.

Algorithm 3 TLDM

1: **Initialize** $l \leftarrow 0$ and $\boldsymbol{d}_r^0$.
2: $[\boldsymbol{m}_i^{z,L}]_{i\in\mathcal{I}} = ULC(\boldsymbol{d}_r^l)$ [15].
3: $[\hat{\boldsymbol{m}}_i^z, \hat{\boldsymbol{C}}_i, \hat{\boldsymbol{T}}_i]_{i\in\mathcal{I}} = LLC([\boldsymbol{m}_i^{z,L}]_{i\in\mathcal{I}}, \boldsymbol{d}_r^l)$(**Algorithm** 1-2).
4: If $\hat{\boldsymbol{T}}^i \geq T_i^{\min}$, then stop, otherwise continue.
5: Update ventilation rate $\boldsymbol{d}_r$:

$$\boldsymbol{d}_r^{l+1}(k) = \boldsymbol{d}_r^l(k) - \Delta d_r \mathbb{I}(\hat{\boldsymbol{T}}_i(k+1) < T_i^{\min}),\ \forall k \in \mathcal{H}.$$

6: Set $l \rightarrow l+1$ and go to **Step** 2.

be achieved along the computing epoch. We illustrate the feasibility issue by induction. For notation, we indicate the real zone CO_2 trajectories as $[C_{i,t}]_{t\in\mathcal{T}}$ $(\forall i \in \mathcal{I})$, which is supposed to be obtained at the end of optimization horizon $\mathcal{T}$. At each execution instant t, we can obtain the current zone CO_2 measurements $C_i(0) = C_{i,t}$ $(\forall i \in \mathcal{I})$. Suppose that at time t, we have $C_{i,t} \leq C_i^{\max}$ $(\forall i \in \mathcal{I})$, and it suffices to address the feasibility issue by proving $C_{i,t+1} \leq C_i^{\max}$ $(\forall i \in \mathcal{I})$ as follows:

$$\begin{aligned} C_{i,t+1} &= C_i(1) \\ &= C_i(0) + E_i(0)\hat{m}_i^z(0) + F_i(0)\hat{m}_i^z(0)C_i(0) + G_i(0) \\ &= C_i(0) + E_i(0)m_i^{z,*}(0) + F_i(0)m_i^{z,*}(0)C_i(0) + G_i(0) \\ &= C_i(0) + E_i(0)m_i^{z,*}(0) + F_i(0)Z_i^*(0) + G_i(0) \\ &\leq C_i^{\max} \quad \forall i \in \mathcal{I} \end{aligned}$$

where the first two equalities are directly from zone CO_2 dynamics (13). The third and fourth equalities are derived from $\hat{m}_i^z(k) = m_i^{z,*}(k)$ and (13a). The inequality is deduced from constraint (8).

Second Phase of LLC: As discussed previously, it may occur that the lower comfortable zone temperature bounds may be violated for solving problem $(\mathcal{P}_L)$. In such a situation, we are required to invoke the second phase of LLC to increase the ventilation rate (decrease d_r). In principle, the regulating step size should be determined by the temperature violation amplitude; however, it is difficult to coordinate such two different dimensions and we thus use a small constant step size Δd_r. The overall framework of the proposed TLDM that embeds the ULC and LLC is presented in Algorithm 3. We use l to denote the iteration. Function $\mathbb{I}(A)$ is an indicator function, where we have $\mathbb{I}(A) = 1$ with true condition A; otherwise, $\mathbb{I}(A) = 0$.

V. Application

We evaluate the performance of the TLDM on multizone commercial HVAC system via simulations. We first study the energy-saving performance and computational advantage of the method via a benchmark (five zones). After that, the capability and scalability of the method to medium-scale (10 and 20 zones) and large-scale (50 and 100 zones) are illustrated.

A. Benchmark

This section considers a five-zone benchmark. We select the general comfortable zone temperature range $[24, 26]$ °C and zone CO_2 range $[0, 800]$ ppm. The set-point temperature of AHU is $T_c = 15$ °C. We assume that the zones are spatially next to each other $1 \leftrightarrow 2 \leftrightarrow 3 \leftrightarrow 4 \leftrightarrow 5 \leftrightarrow 1$. The initial zone temperature is set as $[29, 30, 31, 30, 29]$ °C (zones 1–5). The predicted outdoor temperature and zone occupancy are shown in Fig. 3. The HVAC's energy cost is calculated according to the time-of-use (TOU) price in Singapore [7]. The other parameters refer to Table I.

In the benchmark, we compare the proposed method with: 1) distributed token-based scheduling strategy (DTBSS) [5]; 2) centralized method; 3) the commonly used

TABLE I
SIMULATION PARAMETERS

Param.	Value	Units
$C_i (i \in \mathcal{I})$	1.5×10^3	kJ K^{-1}
c_p	1.012	kJ/kg $-$ K
R_{oi}	50	kW K^{-1}
$R_{ij} (i, j \in \mathcal{I})$	14	kW K^{-1}
κ_f	0.08	-
η	1	-
C_g	40	g h^{-1}
Δd_r	0.05	-
$m_i^{z,\min}$	0	kg h^{-1}
$m_i^{z,\max}$	0.5	kg h^{-1}

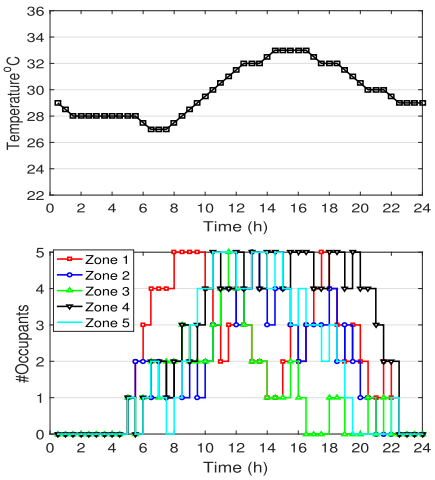

Fig. 3. (a) Outdoor temperature. (b) Zone occupancy.

TABLE II
PERFORMANCE COMPARISONS

Method	R_p	R_a (L/p)	Cost (L/m^2)	Time (s)	TC	IAQ
DTBSS	-	-	245.03	2.11	**Y**	**N**
Centralized	-	-	247.15	575.07	**Y**	**Y**
SQP	-	-	275.91	151.26	**Y**	**Y**
DCV I	21	0	276.23	-	**Y**	**Y**
DCV II	16	0.04	274.99	-	**Y**	**Y**
TLDM	-	-	257.02	5.21	**Y**	**Y**

N=No, **Y**=Yes.

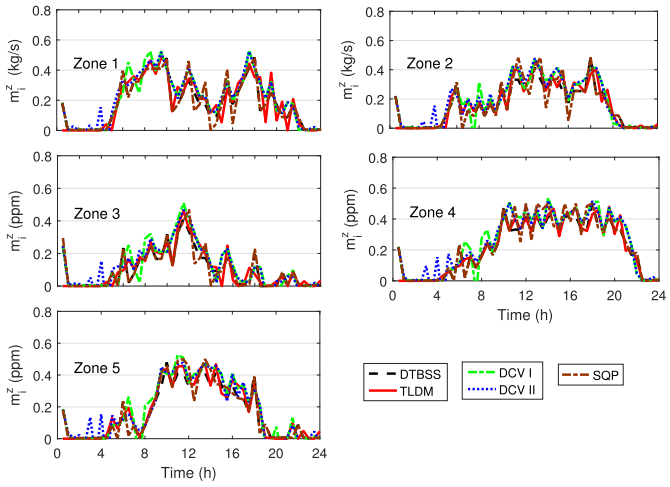

Fig. 4. Zone mass flow rate (Benchmark).

DCV strategies [25], [34]; and 4) sequential quadratic programming (SQP) [35]. Akin to most existing works, the DTBSS lacks IAQ management [5] and we therefore fix the ventilation rate in DTBSS as $d_r(k) = d_r^{\max}$ $(\boldsymbol{k} \in \mathcal{H})$ to achieve the energy cost saving target. For the centralized method, we obtain the optimal solution by solving the nonlinear optimization problem $(\mathcal{P})$ using the IPOPT solver embedded in MATLAB [36]. The DCVs calculate the amount of fresh air by the zone occupancy and zone area [25], [34], that is

$$m_i^{z,\text{fresh}}(k) = N_i(k)R_p + A_i R_a \ \forall k \in \mathcal{H} \tag{20}$$

where A_i denotes the area of zone i and R_p and R_a denote the average occupancy and space ventilation rate, respectively. This article considers two DCVs: 1) DCV I: calculating zone fresh air flow rates based on zone occupancy ($R_p \geq 0$, $R_a = 0$) and 2) DCV II: computing zone fresh air flow rates by zone occupancy and space ($R_p \geq 0$, $R_a \geq 0$).

For single-zone case, the ventilation rate (d_r) of DCVs can be straightforwardly determined by the fresh air infusion and mass flow rate. Nevertheless, for multizone case, the calculation of ventilation rate needs to account for zone diversity [25]

$$\begin{aligned} m^{z,\text{fresh}}(k) &= \sum_{i\in\mathcal{I}} m_i^{z,\text{fresh}}(k), \ m^z(k) = \sum_{i\in\mathcal{I}} m_i^z(k) \\ Z(k) &= \max_{i\in\mathcal{I}} \left\{ \frac{m_i^{z,\text{fresh}}(k)}{m_i^z(k)} \right\}, \quad X(k) = \frac{m^{z,\text{fresh}}(k)}{m^z(k)} \\ Y(k) &= \frac{X(k)}{1+X(k)-Z(k)}, \quad d_r(k) = 1 - Y(k) \ \ \forall k \in \mathcal{H}. \end{aligned} \tag{21}$$

One critical issue to be noticed is that the DCVs only account for IAQ by determining the amounts of fresh air infusion, and the TC that corresponds to the zone mass flow rates is not considered. Therefore, we use the ULC of TLDM to calculate zone mass flow rates $m_i^z(k)$ in DCVs for fair comparisons. Therefore, similar to our TLDM, the DCVs correspond to two alternative procedures: obtain the zone mass flow rates by solving problem $(\mathcal{P}_U)$ (start with $d_r(k) = d_r^{\max}$) and amending the ventilation rate $d_r(k)$ according to (21).

We present the energy cost, average computation time of each computing epoch,[1] satisfaction of TC and IAQ induced by the different methods in Table II. In particular, we exclude the DCVs while studying the computation time as they depend on off-line regulation for the occupancy and space ventilation rates, which is time-consuming. We display the zone mass flow rates, zone temperature, zone CO_2, and ventilation rate in Figs. 4–7. First of all, we find that the zone TC is ensured by each method (see Fig. 5) but not necessary for IAQ (see Fig. 6) as we observe that the desirable zone CO_2 is out of range $[0, 800]$ ppm for DTBSS. This is not surprising as the DTBSS lacks IAQ management. Therefore, the method favors a low ventilation rate (see Fig. 7) to save energy cost and fails to ensure IAQ. Further, we study the energy cost and computational efficiency of different methods. From Table II, we find that the TLDM provides about 7.0% lower energy cost compared with the DCVs and the SQP. Since we observe

[1]MATLAB R2016a on PC with Intel Core i7-5500U CPU at 2.40-GHz processor.

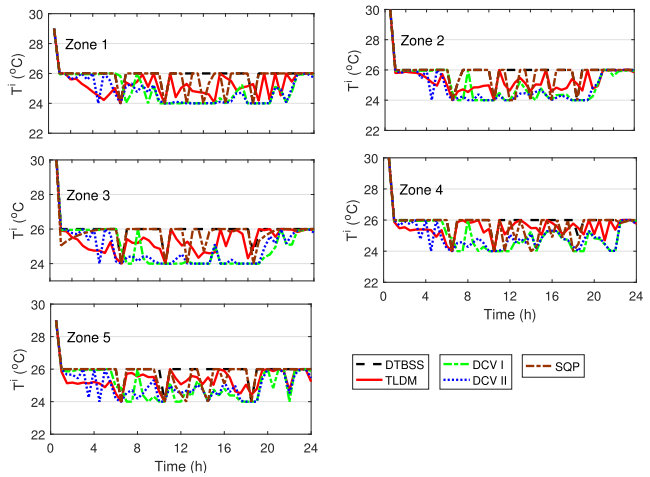

Fig. 5. Zone temperature (Benchmark).

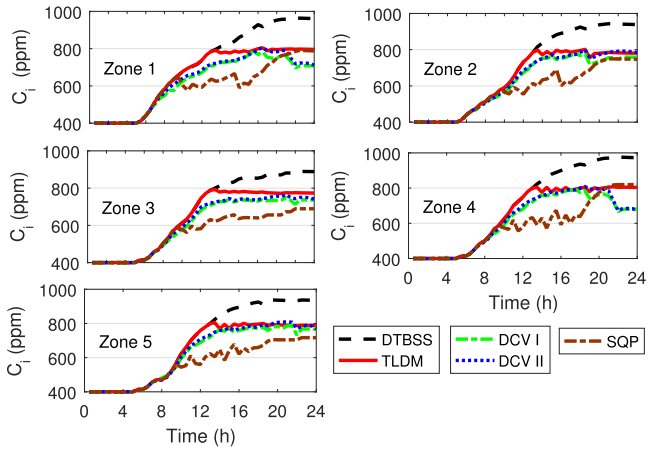

Fig. 6. Zone CO_2 (Benchmark).

close peaks over the zone temperature (see Fig. 5) and zone CO_2 (see Fig. 6) trajectories for these methods, we conclude that the TLDM can maintain the same TC and IAQ but with less energy cost. As for the computational efficiency, the average computation time of TLDM for each executive epoch is about 5.21 s (in parallel) with a slight increase over the DTBSS (2.11 s). This is mainly attributed to the LLC to achieve IAQ. However, the TLDM obviously outperforms SQP in computation efficiency. When compared with the centralized method, we imply the suboptimality of TLDM in energy cost is around 4% in the benchmark. Nevertheless, the computational benefit of TLDM is significant as the average computation time is reduced from 575.07 to 5.21 s.

B. Scalability

In this section, the proposed TLDM is applied to medium (10 and 20 zones) and large (50 and 100 zones) scale cases. Considering that the centralized method and SQP are now computationally intractable, we compare the TLDM with the other three methods (i.e., DTBSS and DCV I and II). For each case, we randomly generate a network to represent the spatial connectivity of the zones (the maximum number of adjacent

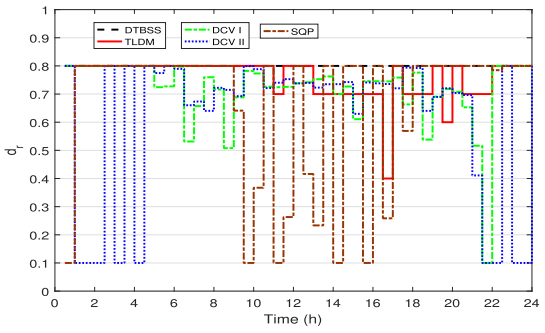

Fig. 7. Ventilation rate $\boldsymbol{d}_r$ (Benchmark).

TABLE III
OCCUPANCY AND SPACE VENTILATION RATES IN DCV I AND II

#zones	DCV I	DCV II	
	R_p (L/p)	R_p (L/p)	R_a (L/m^2)
10	19	15	0.03
20	20	19	0.03
50	21	19	0.03
100	23	21	0.03

TABLE IV
PERFORMANCE COMPARISONS

Method	*Medium*						TC	IAQ
	10			20				
	Cost (s$)	+/- (%)	Time (s)	Cost (s$)	+/- (%)	Time (s)		
TLDM	407.32	-	6.55	939.83	-	8.03	**Y**	**Y**
DTBSS	387.07	-4.97	2.35	887.12	-5.61	2.71	**Y**	**N**
DCV I	447.42	+9.84	-	1015.50	+8.05	-	**Y**	**Y**
DCV II	440.42	+8.13	-	1020.60	+8.59	-	**Y**	**Y**

Method	*Large*						TC	IAQ
	50			100				
	Cost (s$)$\times 10^3$	+/- (%)	Time (s)	Cost (s$)$\times 10^3$	+/- (%)	Time (s)		
TLDM	2.65	-	13.28	5.80	-	21.68	**Y**	**Y**
DTBSS	2.54	-4.15	4.47	5.49	-5.34	6.90	**Y**	**N**
DCV I	2.91	+9.81	-	6.31	+8.79	-	**Y**	**Y**
DCV II	2.92	+10.19	-	6.36	+9.66	-	**Y**	**Y**

N=No, **Y**=Yes.

zones zone is set as 4). In particular, the space and occupancy ventilation rates for the DCVs to achieve the IAQ are shown in Table III, which are obtained from off-line regulation. The other parameters refer to the benchmark in Section IV-A.

Similarly, we investigate the energy cost and computational efficiency of different methods, with the results shown in Table IV. Compared with the DTBSS, we observe a minor increase in energy cost and computation time with the TLDM to achieve IAQ. However, the TLDM is still computationally efficient and scalable by inspecting the average computation time (e.g., 21.68 s for 100-zone case) versus the decision epoch 30 min. Besides, we observe similar gains of the TLDM over the DCVs in energy cost saving: 8.0%–9.8% (DCV I) and 8.1%–10.2% (DCV II). Moreover, except for the energy cost reduction, the TLDM is expected to be more applicable over the DCVs as it does not depend on time-consuming off-line regulation for the occupancy and space ventilation rate.

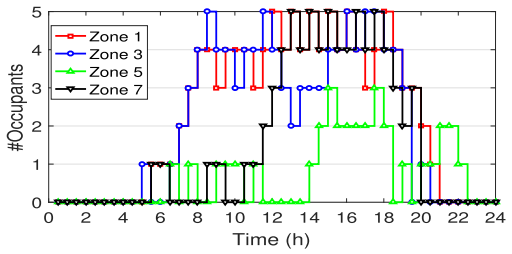

Fig. 8. Dynamic occupancy for the three zones among $I = 50$ zones.

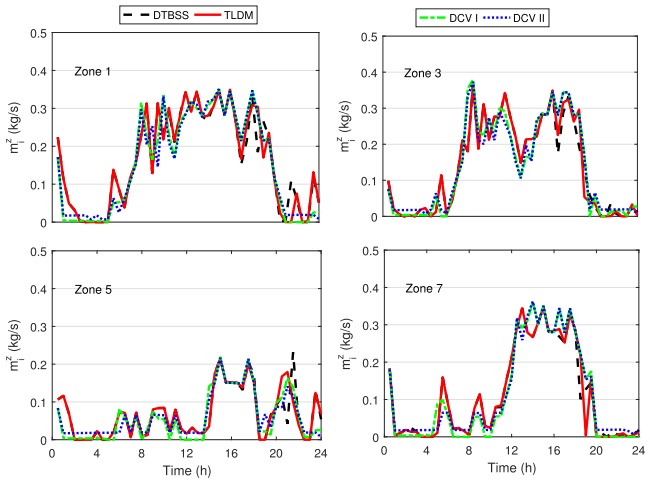

Fig. 9. Zone air flow rates for the three zones among $I = 50$ zones.

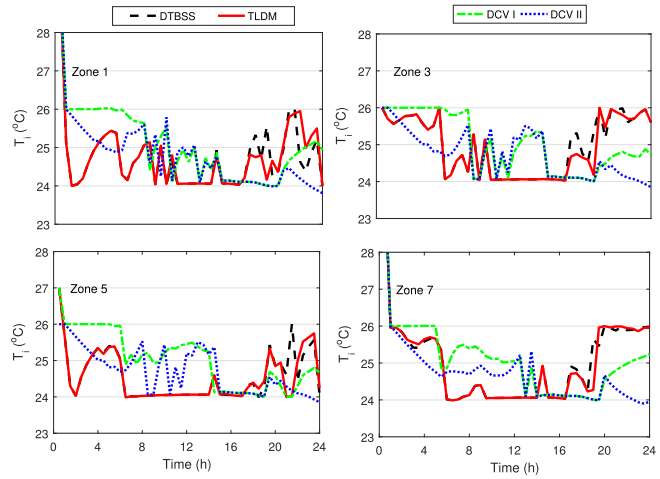

Fig. 10. Temperature for the four zones among $I = 50$ zones.

As an instance, we further investigate the 50-zone case study. We display the zone occupancy, zone mass flow rates, zone temperature, and zone CO_2 for three randomly selected zones in Figs. 8–11. From Figs. 10 and 11, we see that both the TLDM and the DCVs maintain the comfortable zone temperature range ([24, 26] °C) and zone CO_2 range ([0, 800] ppm). Besides, we observe close peak (800 ppm) over the zone CO_2 trajectories under the TLDM and the DCVs, which implies that the close IAQ is maintained by these methods. Besides, from Fig. 10, we can have some insights in the characteristics of the TLDM to achieve TC and IAQ.

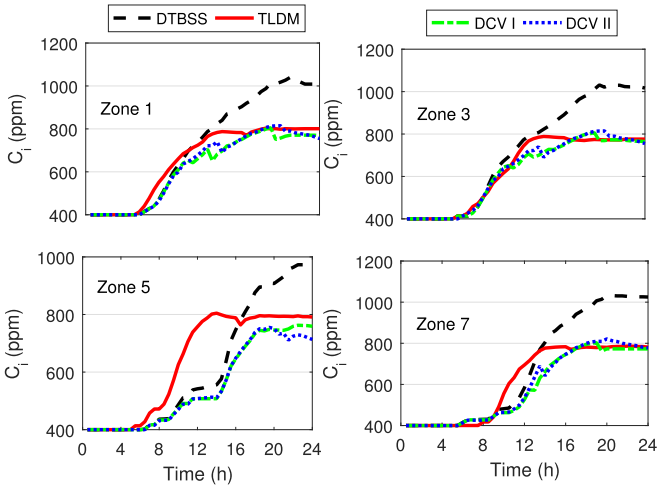

Fig. 11. CO_2 concentration for the four zones among $I = 50$ zones.

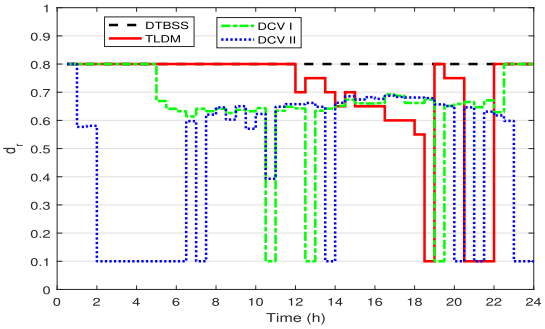

Fig. 12. Ventilation rate ($\boldsymbol{d}_r$) of the HVAC system.

Specifically, we see that the zone temperature approaches the lower bound during the working hours with high occupancy. This phenomenon is caused by the two-phase structure of LLC in TLDM where the zone mass flow rates are first adjusted to achieve IAQ, and then, the ventilation rate is regulated if necessary.

We also compare the ventilation rates ($\boldsymbol{d}_r$) of different methods in Fig. 12, which exhibits some interesting phenomenon to be interpreted. First of all, we see that the ventilation rate of TLDM corresponds well to the occupancy. Specifically, we see a relatively low ventilation rate (larger $\boldsymbol{d}_r$) during the off-working hours but the opposite over the working hours (smaller $\boldsymbol{d}_r$). This is reasonable as the LLC is only invoked to regulate the ventilation rate if the CO_2 is to be violated, which generally results from high occupancy. Surprisingly, the results for DCV I and DCV II are almost opposite and quite different from the TLDM. Specifically, we see that the ventilation rate ($\boldsymbol{d}_r$) of DCV I corresponds well to the occupancy, whereas the DCV II presents the opposite. These phenomena are attributed to the rules that are used to determine zone fresh air flow rates in the DCVs as discussed before. For DCV I, the zone fresh air totally depends on zone occupancy, and thus, we observe a synchronous pace of ventilation rate ($\boldsymbol{d}_r$) with the occupancy. However, for DCV II, the zone mass flow rates are jointly determined by the occupancy and space. Therefore, during the off-working hours with low occupancy, we can

observe a higher ventilation rate as the proportions of zone fresh air flow rates dominate in the total zone mass flows rates (higher proportion) for maintaining TC.

VI. Conclusion

This article studied scalable control of multizone HVAC systems with the objective to reduce the energy cost for maintaining TC and IAQ simultaneously. This problem is computationally challenging due to the complex system dynamics. To cope with the difficulties, we proposed a TLDM that integrates the ULC and LLC by exploiting the problem structures. Specifically, the upper level first optimizes zone mass flow rates to satisfy TC with minimal energy cost and the lower level regulates zone mass flow rates and the ventilation rate to achieve IAQ while preserving the near energy-saving performance of ULC. As both the ULC and LLC use distributed computation, the proposed method is computationally efficient and scalable. The method's performance in energy saving and scalability was demonstrated by numeric studies. The suboptimality of the proposed method in energy cost is around 4% but with significant computational benefits over the centralized method. Compared with the DTBSS, the proposed method induces a marginal increase in energy costs but provides IAQ. In addition, the proposed method provided 8%–10% energy savings over the DCV strategies.

Acknowledgment

BEARS has been established by the University of California, Berkeley, as a center for intellectual excellence in research and education in Singapore.

References

[1] K. L. Ku, J. S. Liaw, M. Y. Tsai, and T. S. Liu, "Automatic control system for thermal comfort based on predicted mean vote and energy saving," *IEEE Trans. Autom. Sci. Eng.*, vol. 12, no. 1, pp. 378–383, Jan. 2015.

[2] H. Mirinejad, K. C. Welch, and L. Spicer, "A review of intelligent control techniques in HVAC systems," in *Proc. IEEE Energytech*, May 2012, pp. 1–5.

[3] A. Afram and F. Janabi-Sharifi, "Theory and applications of HVAC control systems—A review of model predictive control (MPC)," *Building Environ.*, vol. 72, pp. 343–355, Feb. 2014.

[4] A. Kelman and F. Borrelli, "Bilinear model predictive control of a HVAC system using sequential quadratic programming," *IFAC Proc. Volumes*, vol. 44, no. 1, pp. 9869–9874, Jan. 2011.

[5] N. Radhakrishnan, Y. Su, R. Su, and K. Poolla, "Token based scheduling for energy management in building HVAC systems," *Appl. Energy*, vol. 173, pp. 67–79, Jul. 2016.

[6] Y. Yang, G. Hu, and C. J. Spanos, "Stochastic optimal control of HVAC system for energy-efficient buildings," 2019, *arXiv:1911.00840*. [Online]. Available: http://arxiv.org/abs/1911.00840

[7] Z. Xu, G. Hu, C. J. Spanos, and S. Schiavon, "PMV-based event-triggered mechanism for building energy management under uncertainties," *Energy Buildings*, vol. 152, pp. 73–85, Oct. 2017.

[8] H. Dasi, F. Xiaowei, and C. Daisheng, "On-line control strategy of fresh air to meet the requirement of IAQ in office buildings," in *Proc. 5th IEEE Conf. Ind. Electron. Appl.*, Jun. 2010, pp. 845–848.

[9] W. Li, C. Koo, S. H. Cha, T. Hong, and J. Oh, "A novel real-time method for HVAC system operation to improve indoor environmental quality in meeting rooms," *Building Environ.*, vol. 144, pp. 365–385, Oct. 2018.

[10] (2015). *Good Indoor Air Quality Leads to Good Decisions*. Accessed: Dec. 13, 2020. [Online]. Available: https://www.vaisala.com/sites/default/files/documents/VIM-G-HVAC-Good-Indoor-Air-Quality-Application-note-B211681EN.pdf

[11] (2020). *Why Measure CO2 in HVAC Applications*. Accessed: Dec. 13, 2020. [Online]. Available: https://www.co2meter.com/blogs/news/why-measure-co2-hvac-applications

[12] A. Parisio, M. Molinari, D. Varagnolo, and K. H. Johansson, "A scenario-based predictive control approach to building HVAC management systems," in *Proc. IEEE Int. Conf. Autom. Sci. Eng. (CASE)*, Aug. 2013, pp. 428–435.

[13] A. Parisio, D. Varagnolo, M. Molinari, G. Pattarello, L. Fabietti, and K. H. Johansson, "Implementation of a scenario-based MPC for HVAC systems: An experimental case study," *IFAC Proc. Volumes*, vol. 47, no. 3, pp. 599–605, 2014.

[14] L. Yu, D. Xie, C. Huang, T. Jiang, and Y. Zou, "Energy optimization of HVAC systems in commercial buildings considering indoor air quality management," *IEEE Trans. Smart Grid*, vol. 10, no. 5, pp. 5103–5113, Sep. 2019.

[15] Y. Yang, G. Hu, and C. J. Spanos, "HVAC energy cost optimization for a multi-zone building via a decentralized approach," 2019, *arXiv:1905.10934*. [Online]. Available: http://arxiv.org/abs/1905.10934

[16] J. Mei and X. Xia, "Distributed control for a multi-evaporator air conditioning system," *Control Eng. Pract.*, vol. 90, pp. 85–100, Sep. 2019.

[17] C. C. Okaeme, S. Mishra, and J. T.-Y. Wen, "Passivity-based thermo-hygrometric control in buildings," *IEEE Trans. Control Syst. Technol.*, vol. 26, no. 5, pp. 1661–1672, Sep. 2018.

[18] C. C. Okaeme, S. Mishra, and J. T. Wen, "A comfort zone set-based approach for coupled temperature and humidity control in buildings," in *Proc. IEEE Int. Conf. Autom. Sci. Eng. (CASE)*, Aug. 2016, pp. 456–461.

[19] N. Nassif, S. Kajl, and R. Sabourin, "Ventilation control strategy using the supply CO2 concentration setpoint," *HVAC&R Res.*, vol. 11, no. 2, pp. 239–262, Apr. 2005.

[20] T. R. Nielsen and C. Drivsholm, "Energy efficient demand controlled ventilation in single family houses," *Energy Buildings*, vol. 42, no. 11, pp. 1995–1998, Nov. 2010.

[21] A. Hesaraki, J. A. Myhren, and S. Holmberg, "Influence of different ventilation levels on indoor air quality and energy savings: A case study of a single-family house," *Sustain. Cities Soc.*, vol. 19, pp. 165–172, Dec. 2015.

[22] Z. Wang and L. Wang, "Intelligent control of ventilation system for energy-efficient buildings with CO_2 predictive model," *IEEE Trans. Smart Grid*, vol. 4, no. 2, pp. 686–693, Jun. 2013.

[23] N. Nassif, "A robust CO_2-based demand-controlled ventilation control strategy for multi-zone HVAC systems," *Energy Buildings*, vol. 45, pp. 72–81, Feb. 2012.

[24] M. Marinov, T. Djamiykov, B. Ganev, and V. Zerbe, "Sensor-based multi-zone demand-controlled ventilation," in *Proc. INFOTEH-JAHORINA*, vol. 12, Mar. 2013.

[25] K. Shan, Y. Sun, S. Wang, and C. Yan, "Development and *in-situ* validation of a multi-zone demand-controlled ventilation strategy using a limited number of sensors," *Building Environ.*, vol. 57, pp. 28–37, Nov. 2012.

[26] A. Parisio, D. Varagnolo, D. Risberg, G. Pattarello, M. Molinari, and K. H. Johansson, "Randomized model predictive control for HVAC systems," in *Proc. 5th ACM Workshop Embedded Syst. Energy-Efficient Buildings BuildSys*, 2013, pp. 1–8.

[27] Hattersley. *Variable Flow vs Constant Flow*. Accessed: Dec. 20, 2019. [Online]. Available: https://www.hattersley.com/page/hvac/variable-flow-systems

[28] X. Zhang, W. Shi, B. Yan, A. Malkawi, and N. Li, "Decentralized and distributed temperature control via HVAC systems in energy efficient buildings," 2017, *arXiv:1702.03308*. [Online]. Available: http://arxiv.org/abs/1702.03308

[29] Y. Lin, T. Middelkoop, and P. Barooah, "Issues in identification of control-oriented thermal models of zones in multi-zone buildings," in *Proc. IEEE 51st IEEE Conf. Decis. Control (CDC)*, Dec. 2012, pp. 6932–6937.

[30] M. Maasoumy, A. Pinto, and A. Sangiovanni-Vincentelli, "Model-based hierarchical optimal control design for HVAC systems," in *Proc. ASME Dyn. Syst. Control Conf. Bath/ASME Symp. Fluid Power Motion Control*, vol. 1, Jan. 2011, pp. 271–278.

[31] I. Korolija, L. Marjanovic-Halburd, Y. Zhang, and V. I. Hanby, "Influence of building parameters and HVAC systems coupling on building energy performance," *Energy Buildings*, vol. 43, no. 6, pp. 1247–1253, Jun. 2011.

[32] G. P. McCormick, "Computability of global solutions to factorable nonconvex programs: Part—Convex underestimating problems," *Math. Program.*, vol. 10, no. 1, pp. 147–175, 1976.

[33] N. Chatzipanagiotis, D. Dentcheva, and M. M. Zavlanos, "An augmented lagrangian method for distributed optimization," *Math. Program.*, vol. 152, nos. 1–2, pp. 405–434, Aug. 2015.
[34] Z. Sun, S. Wang, and Z. Ma, "*in-situ* implementation and validation of a CO2-based adaptive demand-controlled ventilation strategy in a multi-zone office building," *Numer. Optim. Environ.*, vol. 46, no. 1, pp. 124–133, Jan. 2011.
[35] J. Nocedal and S. J. Wright, "Sequential quadratic programming," *Numer. Optim.*, pp. 529–562, 2006.
[36] Y. Kawajir, C. Laird, and A. Wachter, "Introduction to IPOPT: A tutorial for downloading, installing, and using IPOPT," Carnegie Mellon Univ., Pittsburgh, PA, USA, 2006.

Yu Yang (Student Member, IEEE) received the B.E. degree in automation from the Huazhong University of Science and Technology, Wuhan, China, in 2013, and the Ph.D. degree in automation from Tsinghua University, Beijing, China, in 2018.

She is currently working as a Post-Doctoral Scholar with the Berkeley Education Alliance for Research in Singapore (BEARS), UC Berkeley, Berkeley, CA, USA. Her research interests include decentralized optimization and decision-making, event-based optimization, stochastic optimization (Markov decision process and reinforcement learning), and data-driven analysis/control, with applications to smart buildings, smart grids, and cyberphysical systems.

Seshadhri Srinivasan (Senior Member, IEEE) received the master's degree from Anna University, Chennai, India, in 2005, and the Ph.D. degree from the National Institute of Technology Tiruchirappalli, Tiruchirappalli, India, in 2010.

Since 2015, he has been working with the Berkeley Education Alliance for Research in Singapore (BEARS), Singapore, as a Post-Doctoral Scholar. Prior to this, he was with GRACE, Italy, the Technical University of Munich, Munich, Germany, the Center for Excellence in Nonlinear Systems, Estonia, and the ABB Corporate Research Center, India. He has been a member of the IEEE CSS Standing Committee on standards since 2015 and has served in conferences/workshops. He has published over 50 journal articles and 100 conference papers, authored four books, and patented two technologies.

Guoqiang Hu (Senior Member, IEEE) received the Ph.D. degree in mechanical engineering from the University of Florida, Gainesville, FL, USA, in 2007.

He joined the School of Electrical and Electronic Engineering, Nanyang Technological University, Singapore, in 2011, where he is currently a tenured Associate Professor and the Director of the Centre for System Intelligence and Efficiency. He works on distributed control, distributed optimization, and game theory, with applications to multirobot systems and smart city systems.

Dr. Hu was a recipient of the Best Paper in Automation Award in the IEEE International Conference on Information and Automation and the Best Paper Award (Guan Zhao-Zhi Award) in the 36th Chinese Control Conference. He serves/served as an Associate Editor for the IEEE TRANSACTIONS ON AUTOMATIC CONTROL and the IEEE TRANSACTIONS ON CONTROL SYSTEMS TECHNOLOGY, a Technical Editor for the IEEE/ASME TRANSACTIONS ON MECHATRONICS, and an Associate Editor for the IEEE TRANSACTIONS ON AUTOMATION SCIENCE AND ENGINEERING.

Costas J. Spanos (Fellow, IEEE) received the EE Diploma degree from the National Technical University of Athens, Athens, Greece, and the M.S. and Ph.D. degrees in electrical and computer engineering from Carnegie Mellon University, Pittsburgh, PA, USA.

In 1988, he joined the Department of Electrical Engineering and Computer Sciences (EECS), University of California at Berkeley (UC Berkeley), Berkeley, CA, USA, where he is now the Andrew S. Grove Distinguished Professor and the Director of the Center for Information Technology Research in the Interest of Society (CITRIS) and the Banatao Institute. He is also the Founding Director and CEO of the Berkeley Education Alliance for Research in Singapore (BEARS), and the Lead Investigator of a large research program on smart buildings based in California and Singapore. Prior to that, he has been the Chair of EECS at UC Berkeley, the Associate Dean for Research in the College of Engineering at UC Berkeley, and the Director of the UC Berkeley Microfabrication Laboratory. His research focuses on sensing, data analytics, modeling, and machine learning, with broad applications in semiconductor technologies and cyberphysical systems.